

## Bioinformatic analysis of highly consumed phytochemicals as P-gp binders to overcome drug-resistance

Narges Rajaei<sup>1</sup>, Ghazaleh Rahgouy<sup>1</sup>, Nasrin Panahi<sup>1</sup>, and Nima Razzaghi-Asl<sup>2,3,\*</sup>

<sup>1</sup>Students Research Committee, School of Pharmacy, Ardabil University of Medical Sciences, Ardabil, Iran.

<sup>2</sup>Pharmaceutical Sciences Research Center, Ardabil University of Medical Sciences, Ardabil, Iran.

<sup>3</sup>Department of Medicinal Chemistry, School of Pharmacy, Ardabil University of Medical Sciences, Ardabil, Iran.

### Abstract

**Background and purpose:** P-glycoprotein (P-gp) is an adenosine triphosphate (ATP)-dependent membrane efflux pump for protecting cells against xenobiotic compounds. Unfortunately, overexpressed P-gp in neoplastic cells prevents cell entry of numerous chemotherapeutic agents leading to multidrug resistance (MDR). MDR cells may be re-sensitized to chemotherapeutic drugs *via* P-gp inhibition/modulation. Side effects of synthetic P-gp inhibitors encouraged the development of natural products.

**Experimental approach:** Molecular docking and density functional theory (DFT) calculations were used as fast and accurate computational methods to explore a structure binding relationship of some dietary phytochemicals inside distinctive P-gp binding sites (modulatory/inhibitory). For this purpose, top-scored docked conformations were subjected to per-residue energy decomposition analysis in the B3LYP level of theory with a 6-31g (d, p) basis set by Gaussian98 package.

**Findings/Results:** Consecutive application of computational techniques revealed binding modes/affinities of nutritive phytochemicals within dominant binding sites of P-gp. Blind docking scores for best-ranked compounds were superior to verapamil and rhodamine-123. Pairwise amino acid decomposition of superior docked conformations revealed Tyr303 as an important P-gp binding residue. DFT-based induced polarization analysis revealed major electrostatic fluctuations at the atomistic level and confirmed larger effects for amino acids with energy-favored binding interactions. Conformational analysis exhibited that auraptene and 7,4',7'',4'''-tetra-*O*-methylamentoflavone might not necessarily interact to P-gp binding sites through minimum energy conformations.

**Conclusion and implications:** Although there are still many hurdles to overcome, obtained results may propose a few nutritive phytochemicals as potential P-gp binding agents. Moreover; top-scored derivatives may have the chance to exhibit tumor chemo-sensitizing effects.

**Keywords:** Chemosensitizers; Molecular docking; Multidrug resistance; P-gp; Phytochemicals.

### INTRODUCTION

Permeability glycoprotein (P-gp) is a 170 kDa adenosine triphosphate (ATP)-dependent membrane transporter that protects cells from toxic compounds *via* an efflux mechanism (1). Overexpressed P-gp on the surface of neoplastic cells confines cell entry of drugs and chemotherapeutic agents (2,3). Impaired pharmacological effect due to insufficient intracellular drug concentrations leads to the phenomenon described as multidrug resistance (MDR) of cancer cells (4). It has been

well documented that MDR cells may be chemically sensitized to anticancer drugs *via* P-gp inhibition/modulation (5). In this context, a promising suggestion to overwhelm MDR would be the concomitant administration of anticancer drugs and P-gp inhibitors (6).

#### Access this article online



Website: <http://rps.mui.ac.ir>

DOI: 10.4103/1735-5362.383706

\*Corresponding author: N. Razzaghi-Asl

Tel: +98-4533523833, Fax: +98-4533522197

Email: n.razzaghi@arums.ac.ir

Toxic effects and lack of efficacy of MDR modulators have been previously reported (4). Despite studies on synthetic derivatives (7), a considerable attempt has been made on natural compounds to show their potential as P-gp inhibitors (8). Several natural products are widely consumed by the public through their daily diets and supplements. In this regard, the interactions between dietary phytochemicals and co-administered medications are likely to affect the pharmacokinetics of chemotherapeutic drugs (9). Due to the importance of drug-food interactions, several studies have focused on the binding pattern of diverse phytochemicals to P-gp to find potent inhibitors that enhance the clinical effect of desired drugs (6,10,11). Some phytochemicals have been reported to reduce resistance *via* modulation of the P-gp transport function (12). For instance, limonene has been reported to revert *Haemonchus contortus* tolerance to ivermectin (13). Other data showed that piperine, capsaicin, and [6]-gingerol modulated doxorubicin tissue distribution (9). Moreover, synthetic P-gp inhibitors require high serum concentrations to achieve a pharmacological effect (14). This issue may be solved by adding alternative nutritious phytochemicals.

Several researchers have focused on the *in-silico* modeling of phytochemicals as P-gp binders (4,15). In continuation of our previous study (16), molecular docking and functional B3LYP (Becke, 3-parameter, Lee-Yang-Parr) in association with the 6-31G (d, p) basis set have been exploited consecutively to evaluate the P-gp intermolecular interactions to a few dietary phytochemicals. The aim was to acquire chemical models for describing the binding features of candidate compounds within P-gp complexes and explore the chemosensitizing potential of the studied phytochemicals.

## MATERIALS AND METHODS

### Ligand dataset

Resveratrol, diallyl sulfide, indole-3-carbinol, cinnamaldehyde, eugenol, trans-cinnamyl acetate, nobiletin, auraptene, and

sulforaphane were nominated as dietary phytochemicals for our *in-silico* study. 7,4',7'',4'''-tetra-*O*-methylamentoflavone (10) was selected from a collection of biflavonoid structures (17) on the basis of Swiss-ADME (Absorption, distribution, metabolism, and excretion) driven drug-like properties (18). Candidate structures with their chemical properties are summarized in Table 1.

### Target and molecular docking study

Crystallographic 3-dimensional holo-structure of mouse P-gp (3.50 Å) was retrieved from a protein data bank (4XWK; www.rcsb.org) with %87 sequence identity (19). Ligand-flexible docking was performed by AutoDock 4.2 package (20). Lamarckian genetic algorithm (21) was used to simulate the binding model of phytochemicals inside P-gp binding site. All the processing steps were done according to the previous publication (16). Ligand-receptor binding interactions were predicted and represented by a protein-ligand interaction profiler (PLIP) server (22).

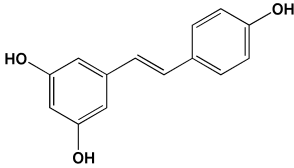
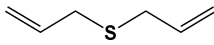
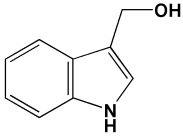
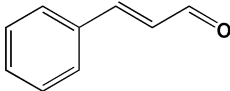
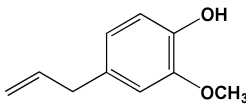
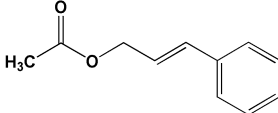
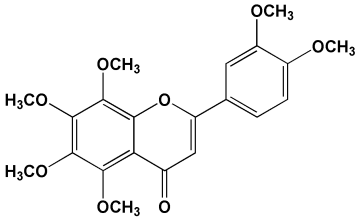
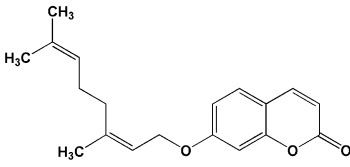
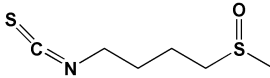
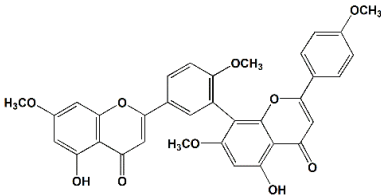
### Density functional theory calculations

Pairwise decomposition of intermolecular binding energy was performed for top-scored docked P-gp complexes. To mimic the real states, the C-terminals and N-terminals of residues were methyl amidated and acetylated, respectively. Polar H-bonds were optimized using a semiempirical PM6 method through heavy atom fixing approximation to obtain the geometry of H-bonds (23). Ligand-residue binding energies were estimated by functional B3LYP in association with a 6-31G (d, p) basis set. The whole calculations were run by the Gaussian 98 quantum chemistry package (24). All ligand-residue binding energies were estimated through Equation 1:

$$\Delta E_{LR} = \Delta E_L - \Delta E_R \quad (1)$$

$E_{LR}$  indicates ligand-residue binding energy.  $E_R$  and  $E_L$  stand for electronic energies of residue and ligand, respectively. Induced polarizabilities were calculated based on Mulliken partial charges of the heavy atoms (25).

**Table 1.** Chemical structures of dietary phytochemicals under study.

Compound name	Natural source	Chemical structure	Molecular weight	HBA	HBD	RTBs	C logp
Resveratrol	Grape		228.08	3	3	2	2.48
Diallyl sulfide	Garlic		114.05	0	0	4	2.14
Indole-3-carbinol	Cabbage		147.07	1	2	2	1.45
Cinnamaldehyde	Cinnamon		132.06	1	0	2	1.97
Eugenol	Clove		164.08	2	1	3	2.25
Trans-cinnamyl acetate	Cinnamon		176.08	2	0	4	2.33
Nobiletin	Citrus peels		402.13	8	0	7	3.02
Auraptene	Citrus fruits		298.16	3	0	6	4.51
Sulforaphene	Broccoli		177.03	2	0	5	1.93
7,4',7'',4'''-tetra-O-methylamentoflavone	Araucaria columnaris		594.15	10	2	7	5.01

HBA, Hydrogen bond acceptor; HBD, hydrogen bond donor; RTB, rotatable bond; C logp, calculated logp.

## RESULTS

### Molecular docking

The validation of the docking protocol for the prediction of binding poses and energy was demonstrated in terms of root mean square deviation (RMSD;  $< 2 \text{ \AA}$ ) from co-crystallographic ligand (RMSD:  $0.934 \text{ \AA}$ ).

Docking studies were performed to identify essential interacted residues of the P-gp. For this purpose, docking space was divided into different boxes including modulator site (M) and substrate sites (R and H), and candidate phytochemicals (Compounds **1-10**) were discretely docked into the designated binding sites. Binding scores of phytochemicals were described as mean binding energies of the most populated top-ranked cluster for each binding site (M, H, and R; Table 2). Free energy coefficients were set at 0.1662, 0.1209, 0.1406, 0.1322, and 0.2983 for van der Waals, H-bonding, electrostatic, desolvation, and torsional terms of the force field, respectively.

### Blind docking

To ensure the validity of binding pockets, blind docking was used to scan the entire P-gp binding site in the presence of phytochemicals. For this purpose, the whole internal binding site was designed as a single grid box ( $126 \times 126 \times 126 \text{ \AA}^3$ ) without any prior knowledge of precise drug binding pockets. All

other parameters were held constant. Nearly close binding scores to prior docking results (site-oriented docking protocol) could be obtained for almost all of the compounds (Table 2). It was interestingly observed that diallyl sulfide, indole-3-carbinol, cinnamaldehyde, and trans-cinnamyl acetate exhibited equal binding energies in two docking protocols. Nobiletin was the sole compound that noticeably exhibited divergent binding energies ( $\Delta G_b$  -6.72 and -7.84 kcal/mol). On the basis of top-ranked binding poses (Fig. 1A-L), resveratrol was accommodated in R-site (Fig. 1A). Binding poses of diallyl sulfide, indole-3-carbinol and cinnamaldehyde was approximately superimposed on each other (Fig. 1B-D). Unlike eugenol (Fig. 1E), binding poses of trans-cinnamyl acetate (Fig. 1F) had also good compatibility. For nobiletin, binding regions were apart from each other in confirmation of docking scores (Fig. 1G). Auraptene favorably binds to the M-site (Fig. 1H) but, sulforaphane binds to the M and R-sites simultaneously (Fig. 1I). 7,4',7'',4'''-tetra-*O*-methylamentoflavone interacted with similar sites but on the basis of binding poses, it could be designated as a P-gp substrate rather than a modulatory (Fig. 1J). For verapamil, predicted binding poses indicated preferential accommodation into the communal region of R- and M-sites (Fig. 1K). Rhodamin was resided in R-site (Fig. 1L).

**Table 2.** Results of docked phytochemicals into different binding sites of P-glycoprotein (PDB ID: 4XWK).

Compound code	Compound	Estimated binding free energy (kcal/mol) (Site-oriented docking)			Estimated binding free energy (kcal/mol) (Blind docking)
		Modulator site	Substrate site (Hoechst 33342)	Substrate-site (Rhodamine-123)	
1	Resveratrol	-6.71	-5.60	-6.79	-6.82
2	Diallyl sulfide	-3.28	-2.89	-3.78	-3.78
3	Indole-3-carbinol	-5.14	-4.63	-5.87	-5.85
4	Cinnamaldehyde	-4.90	-4.90	-5.73	-5.72
5	Eugenol	-4.64	-4.87	-5.22	-5.13
6	Trans-cinnamyl acetate	-5.51	-4.81	-6.05	-6.04
7	Nobiletin	-6.72	-6.36	-6.34	-7.84
8	Auraptene	-7.94	-6.74	-7.56	-8.10
9	Sulforaphane	-4.20	-3.72	-5.17	-5.08
10	7,4',7'',4'''-Tetra- <i>O</i> -methyl amentoflavone	-9.47	-8.82	-9.46	-9.24
11	Verapamil	-7.55	-	-	-7.71
12	Hoechst 33342	-	-8.14	-	-9.66
13	Rhodamine-123	-	-	-7.68	-7.93

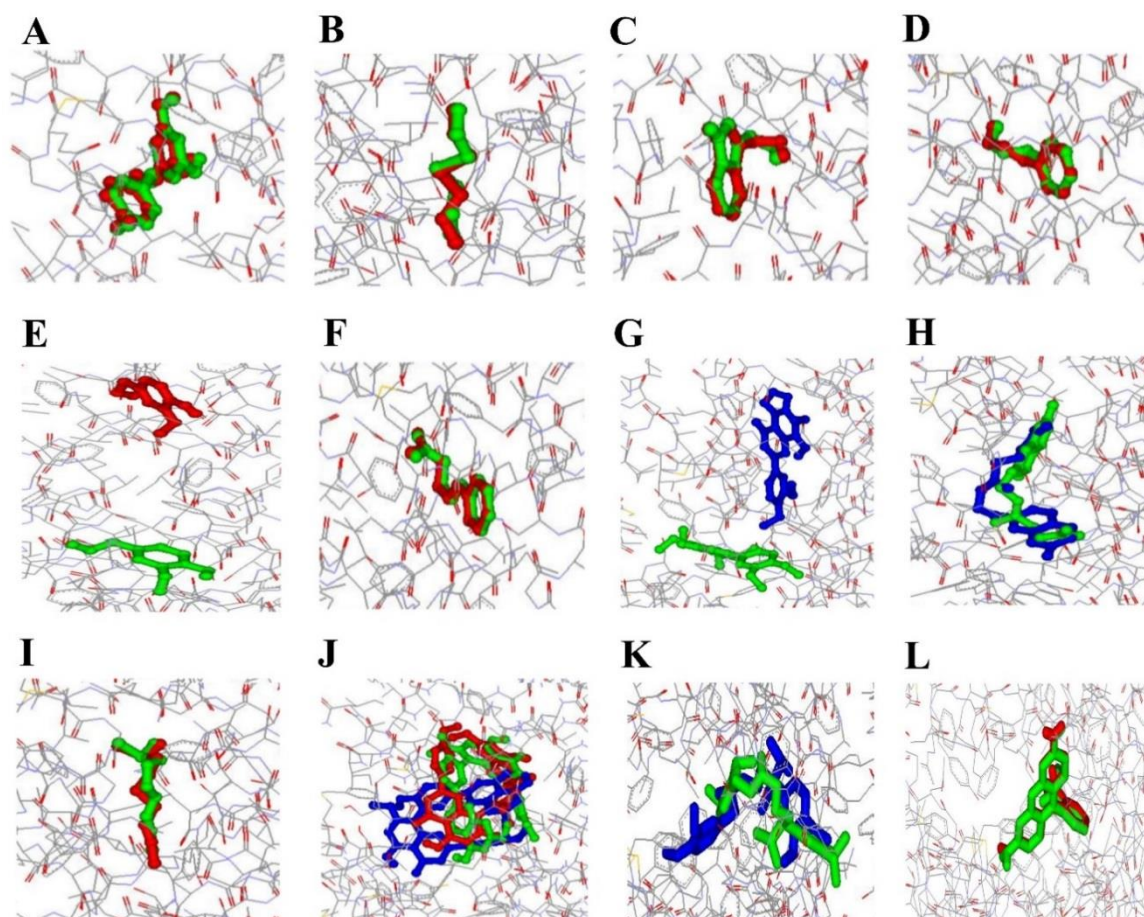


**Fig. 1.** Top-ranked binding poses of phytochemicals within site-directed (R- and M-sites) and blind docking into P-glycoprotein, R-site (red), M-site (blue) and blind docking (green). (A) resveratrol (R-site); (B) diallyl sulfide (M- and R-sites); (C) indole-3-carbinol (R-site), (D) cinnamaldehyde (R-site); (E) eugenol (green: R- and M-site; red: R-site); (F) trans-cinnamyl acetate (R-site); (G) nobiletin (green: M-site; red: R and M-site); (H) auraptene (M-site); (I) sulforaphane (M and R-sites); (J) 7,4',7'',4'''-tetra-*O*-methylamentoflavone (M and R-sites); (K) verapamil (M-site); and (L) rhodamine-123 (R-site). M-site, modulator site; R and H, substrate sites for Hoechst 33342 and Rhodamine-123.

### **Pairwise energy decomposition**

In spite of beneficial features, docking offers no information on distinct ligand-amino acid binding energies in the target site. Density functional theory (DFT) calculation is a complementary approach to molecular docking. It is capable of decomposing intermolecular energies to reveal dominant interacted residues. The contribution of distinct amino acids in binding to a typical ligand is very important in pharmacophore design. We were prompted to estimate the binding energies between top-scored phytochemicals and P-gp residues. For this purpose, auraptene/P-gp and 7,4',7'',4'''-tetra-*O*-methylamentoflavone/P-gp complexes were designated as model systems for pairwise energy analysis.

### **Auraptene**

Our results did not exhibit any H-bonds in the

binding pattern of auraptene to the P-gp M-site. It seems that docked complex was accommodated solely through hydrophobic contacts (Fig. 2A). A few carbon atoms of Phe755 were involved in non-polar interactions to auraptene alkyl substituent ( $\Delta E_b$  -2.56 kcal/mol). A characteristic structural feature of auraptene is the presence of an alkyl substituent (3,7-dimethylocta-2,6-dienyloxy) of the chromenone ring. The alkyl chain participated in hydrophobic contacts to Phe331, Phe755, Ala307, and Ile727 side chains. The hydrophobic contribution of Phe331 and Tyr303 were supported by -0.02 and -2.38 kcal/mol, respectively. It was also revealed that Ala307 (0.98 kcal/mol), Phe724 (1.34 kcal/mol), and Ile727 (0.06 kcal/mol) were not energy-favored contributing residues (Fig. 2B).

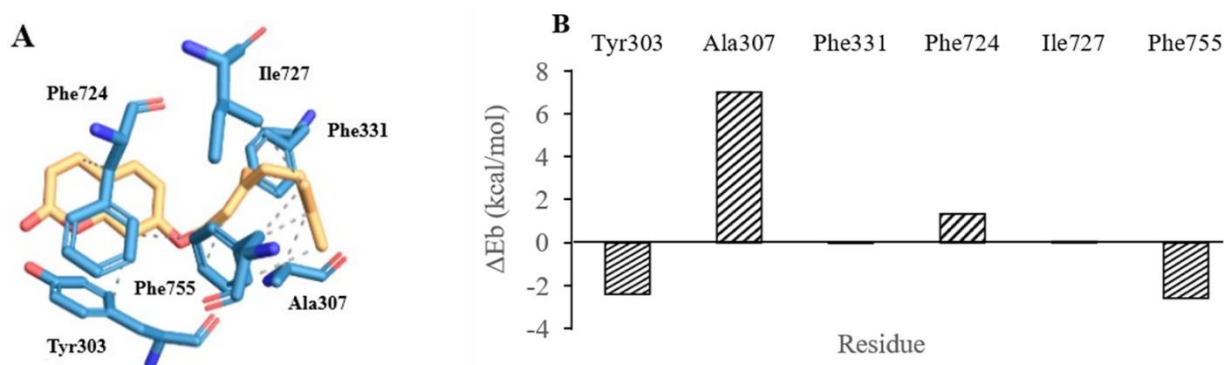


**Fig. 2.** (A) AutoDock 4.2 driven binding interactions and (B) relevant density functional theory calculated ligand-residue binding energies at B3LYP level for auroaptene / P-glycoprotein complex (PDB ID: 4XWK).

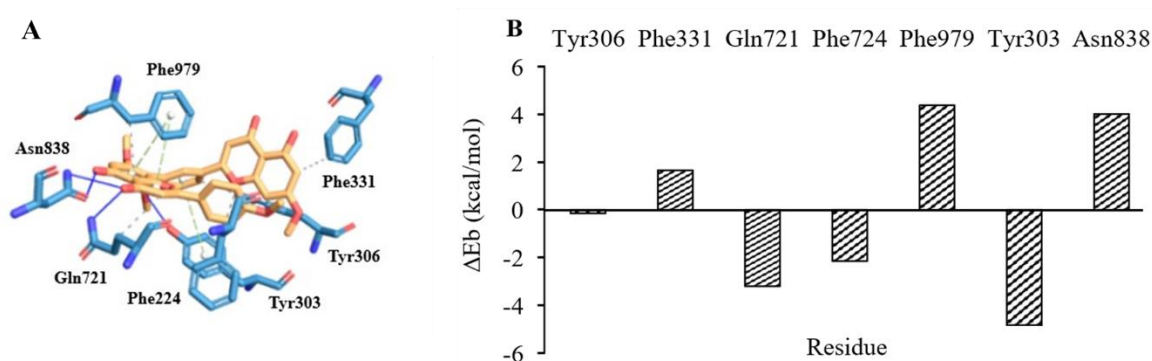


**Fig. 3.** (A) AutoDock 4.2 driven binding interactions and (B) relevant density functional theory calculated ligand-residue binding energies at B3LYP level for 7,4',7'',4'''-tetra-O-methylamentoflavone/P-glycoprotein complex (PDB ID: 4XWK).

### 7,4',7'',4'''-tetra-O-methylamentoflavone

It has been well revealed that more polar residues are dominantly present in P-gp substrate sites. Detailed binding interactions of 7,4',7'',4'''-tetra-O-methylamentoflavone showed participation of H-bond and hydrophobic contacts in complex formation (Fig. 3A). Tyr303, Gln721, and Asn838 were H-bond interacted residues. DFT calculations estimated considerable binding contribution for Tyr303 ( $\Delta E_b$  -4.82 kcal/mol; Fig. 3B). Besides H-bond interaction between Tyr303 side chain hydroxyl and methoxy group of the central phenyl ring,  $\pi$ -stacking contact could also be observed between phenyl rings. The distance between ring centers was estimated to be 5.02 Å with T-shaped geometry of  $\pi$ -stacking. Gln721 was another P-gp residue with significant binding energy (-3.20 kcal/mol) that resided in the R-pocket entrance. Binding patterns showed that Gln721 backbone NH contributed to H-bond with the carbonyl group of a chromenone ring. Gln721 side chain and the carbon atom of chromenone ring also made hydrophobic contact. Phe724 showed energy-

favoured hydrophobic interaction and the total binding contribution of the residue was estimated to be -2.15 kcal/mol. Tyr306 emerged as a weak hydrophobic participant (-0.15 kcal/mol) (Fig. 3B).

### Verapamil

On the basis of DFT calculations, the binding pattern of verapamil showed more energy-favorable interactions in comparison to other ligand/P-gp models (Fig. 4A and B). It seems that the cooperative effect of hydrophobic contributions was a determinant in complex formation. Tyr306 was the best-ranked interacted residue ( $\Delta E_b$  -1.34 kcal/mol). A weak  $\pi$ -stacking interaction was detected between the Phe755 side chain phenyl and verapamil dimethoxy phenyl ring ( $\Delta E_b$  -0.05 kcal/mol). The distance between ring centers was found to be 4.30 Å and the geometry of  $\pi$ -stacking contact was P-shaped. Moreover; our B3LYP level of calculation could not assign perceptible binding energy to the cation- $\pi$  interaction Tyr303 and verapamil protonated amine ( $\Delta E_b$  -0.01 kcal/mol).

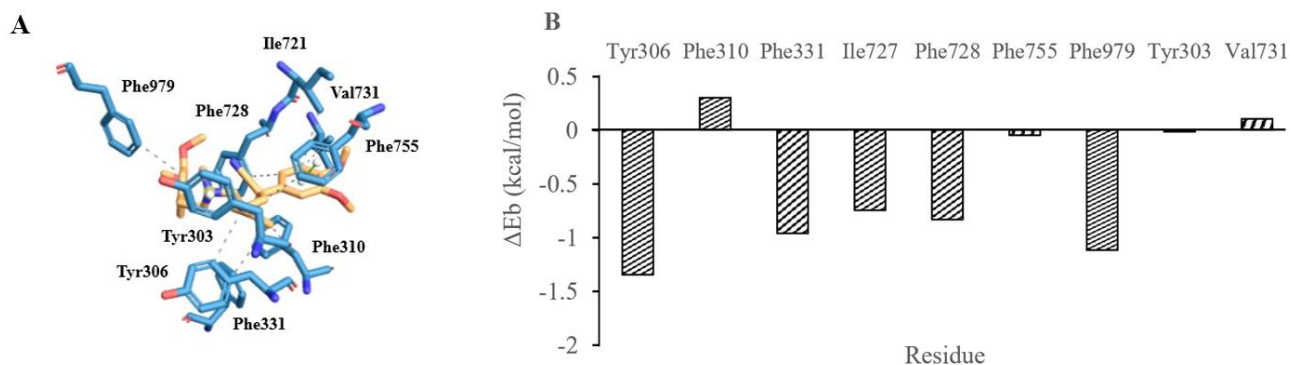


**Fig. 4.** (A) AutoDock 4.2 driven binding interactions and (B) relevant density functional theory calculated ligand-residue binding energies at B3LYP level for verapamil / P-glycoprotein complex (PDB ID: 4XWK).

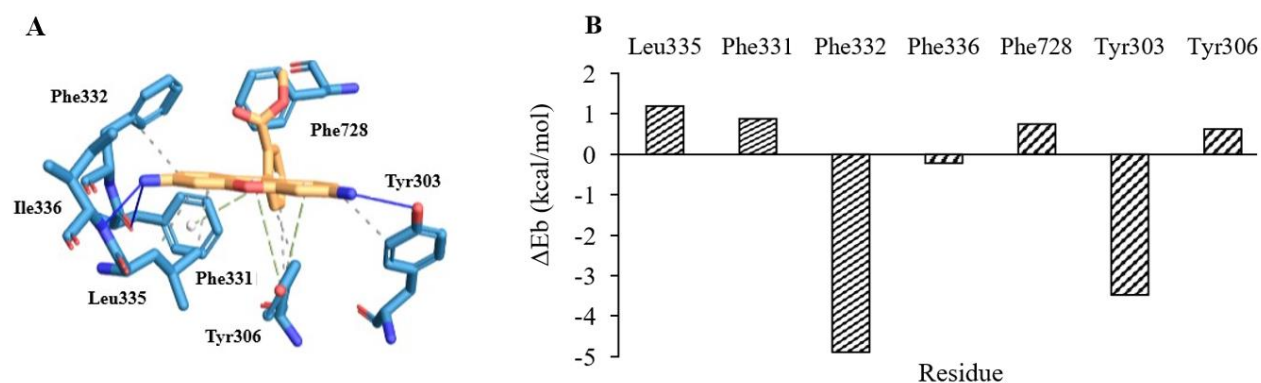


**Fig. 5.** (A) AutoDock 4.2 driven binding interactions and (B) relevant density functional theory calculated ligand-residue binding energies at B3LYP level for rhodamine-123 / P-glycoprotein complex (PDB ID: 4XWK).

### Rhodamine-123

In confirmation of the previous results on the more polar characteristic of P-gp substrate sites, the rhodamine-123 complex was mediated by both H-bond and hydrophobic interactions (Fig. 5A). Phe332 was the best-ranked contributed hydrophobic residue (-4.88 kcal/mol). Ile336 backbone nitrogen served as an H-bond acceptor to the rhodamine amine group. The binding energy of -0.22 kcal/mol was estimated for the overall contribution of Ile336 (Fig. 5B). Tyr303 was an energy-favored residue in binding to compounds 8 and 10. In the case of rhodamine, the overall contribution of the residue was supported by -3.47 kcal/mol. This might be attributed to the positive cooperation of hydrophobic and polar interactions of the Tyr303 side chain. H-bond interaction between Tyr303 side chain oxygen and rhodamine-123 amine group showed

appropriate geometry. The distance between donor and acceptor atoms was 3.15 Å and the donor-acceptor-hydrogen angle was 161.45°. Tyr303 could be regarded as an important residue of the P-gp binding site in binding to phytochemicals. Despite the participation of Tyr306 and Phe331 in T-shaped  $\pi$ -stacking interactions with the aromatic rings of rhodamine-123, no energy-favored binding contributions could be predicted for these amino acids.

P-gp comprises three putative binding sites that have been designated as M (modulator site), H and R (substrate site) (26,27). R-site contains a cytoplasmic inner leaflet C-terminal position whereas, H-site is deeply buried in the cytoplasmic leaflet of the membrane (26). The approximate locations of designated binding sites are depicted in Fig. 6 (16).

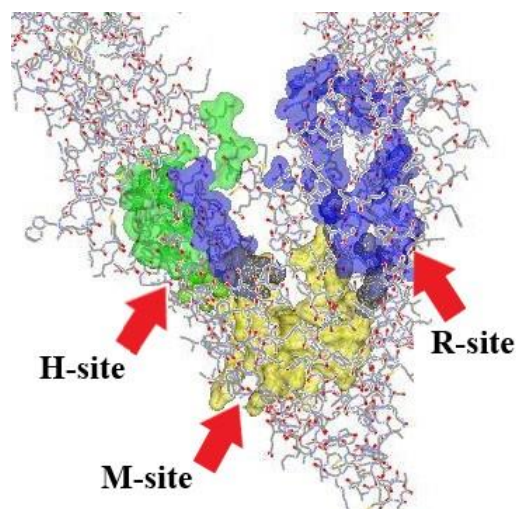


**Fig. 6.** Approximate locations of M-, R-, and H-sites of P-glycoprotein re-generated on the basis of macromolecular 3D structure (PDB 4XWK). Yellow: M-site, blue: R-site, and green: H-site. M-site, modulator site; R and H, substrate sites for Hoechst 33342 and Rhodamine-123.

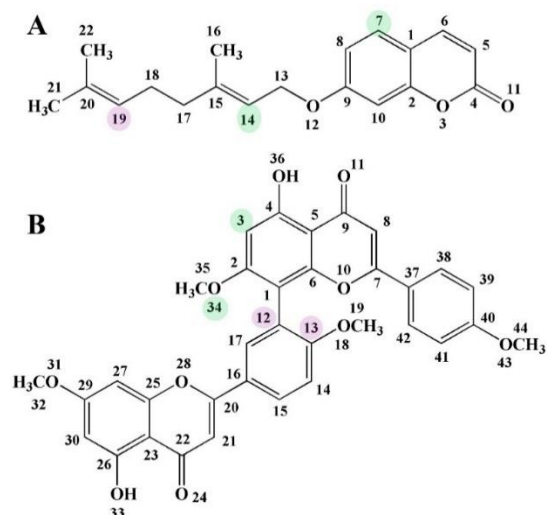


**Fig. 7.** Chemical structures of (A) auraptene and (B) 7,4',7'',4'''-tetra-O-methylamentoflavone, highest and lowest induced polarizability values upon binding to P-glycoprotein residues were respectively designated by red and green ovals. C3, 7,4',7'',4'''-tetra-O-methylamentoflavone-Tyr306/Phe724/Phe331; C7, auraptene-Phe755; C12, 7,4',7'',4'''-tetra-O-methylamentoflavone-Tyr306/Phe724/Phe331; C13, 7,4',7'',4'''-tetra-O-methylamentoflavone-Tyr303; C14, auraptene-Tyr303/Phe331; C19, auraptene-Tyr303/Phe331/Phe755; and O34, 7,4',7'',4'''-tetra-O-methylamentoflavone-Tyr303.

**Table 3.** The sum of squared Mulliken charges for various phytochemicals induced by energy-favored interacted residues of P-gp binding site.

Ligand-target complex	Inducing P-gp residue	qi <sup>2</sup> a	qj <sup>2</sup>	Δ(q <sup>2</sup> ) b
Auraptene - P-gp	Tyr303	3.36	1.98	1.39
Auraptene - P-gp	Phe331	3.36	1.97	1.39
Auraptene - P-gp	Phe755	3.36	1.20	2.16
7,4',7'',4'''-tetra-O-methyl amentoflavone - P-gp	Tyr303	6.66	3.75	2.91
7,4',7'',4'''-tetra-O-methyl amentoflavone - P-gp	Tyr306	6.66	3.75	2.91
7,4',7'',4'''-tetra-O-methyl amentoflavone - P-gp	Gln721	6.66	3.78	2.89
7,4',7'',4'''-tetra-O-methyl amentoflavone - P-gp	Phe724	6.66	3.76	2.91

P-gp, P-glycoprotein; a, Sum of squared partial charges in optimized ligand; b, sum of squared partial charges in optimized ligand – sum of squared partial charges in the docked ligand.

### Induced polarizability

A dominant portion of the stereoelectronic effect could be attributed to the ligand polarizability induced by distinct P-gp residues. We were prompted to explore the stereoelectronic effects of interacted P-gp residues on phytochemicals at an atomistic level. For this purpose, Mulliken partial charges of the heavy atoms of the best-ranked binding poses were estimated and used to determine the inducing effect of each interacted residue on a docked ligand (Fig. 7). Ligand-induced polarizability (IP) can be defined as the difference between the sum of squared partial

charges inbound (docked) and unbound (geometrically optimized) states ( $\Delta q^2$ ) for each phytochemical (equation 2):

$$\Delta q^2 = \sum q_i^2 - \sum q_j^2 \quad (2)$$

In the abovementioned equation,  $q_i$  and  $q_j$  are the partial charges of distinct atoms of each phytochemical in the absence (unbound) and presence (bound) of interacted P-gp residue, respectively. The larger  $\Delta q_2$  is indicative of higher induction and hence more electrostatic participation in binding interactions. The relevant IP effects are summarized in Table 3.



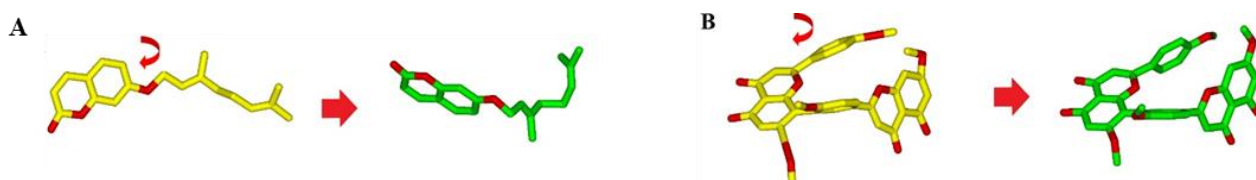


**Fig. 8.** Conformational shift of (A) auraptene and (B) 7,4',7'',4'''-tetra-O-methylamentoflavone from optimized (unbound) to docked states upon binding to P-glycoprotein binding site (major dihedral rotations are designated).

### Conformational analysis

The difference between ligand electronic energies in the optimized and docked conformers may be indicative of ligand conformational instability upon binding to the receptor. Different energies of ligand conformations may be a direct outcome of varied internal energies of ligand in its docked and optimized conditions ( $\Delta E_{\text{instability}}$ ).  $\Delta E_{\text{inst}}$  may be related to the free energy of binding via the following equations:

$$\Delta G_b = \Delta H_b - T\Delta S_b \quad (3)$$

$$\Delta H_b = \Delta E_t - P\Delta V \approx \Delta E_{tb} \quad (4)$$

$$\Delta E_{tb} = \Delta E_b + \Delta E_{\text{inst}} \quad (5)$$

Higher  $\Delta E_{\text{inst}}$  values lead to more positive total binding energies ( $\Delta E_{tb}$ ). The outcome would be weaker ligand-receptor interactions ( $\Delta G_b$ ). Our B3LYP level of energy calculation revealed that auraptene tolerated 25.64 kcal/mol conformational instability upon binding to P-gp M-site. This may be indicative of a noticeable torsional shift toward a less stable conformational pose ( $\Delta E_{\text{inst}}$  of 25.64 kcal/mol). 7,4',7'',4'''-tetra-O-methylamentoflavone showed less stability loss upon binding to M/R-sites ( $\Delta E_{\text{inst}}$  of 6.70 kcal/mol). Conformational shift of (A) auraptene and (B) 7,4',7'',4'''-tetra-O-methylamentoflavone from optimized (unbound) to docked states upon binding to P-glycoprotein binding site (major dihedral rotations are designated) are depicted in Fig. 8.

## DISCUSSIONS

Results showed that unlike nobiletin, auraptene, and 7,4',7'',4'''-tetra-O-methylamentoflavone with tighter interactions to M-site, other phytochemicals showed higher binding scores in R-site and hence might be classified as P-gp substrate. Due to the close binding energies and cluster populations in interaction to R and M-sites, resveratrol, and 7,4',7'',4'''-tetra-O-methylamentoflavone might not be easily discriminated as P-gp modulator or substrate.

In accordance with the more hydrophobic nature of M-site (27), our computational results showed a determinant role of fused aromatic rings of nobiletin, auraptene, and 7,4',7'',4'''-tetra-O-methylamentoflavone in binding to P-gp M-site. In this regard, ethyl acetate extract of nobiletin has been previously demonstrated to increase steady-state vinblastine uptake by LLC-GA5-COL300 cells (transformant cells of drug-sensitive epithelial cells) via inhibiting P-gp (28). Enhanced accumulation of daunorubicin in KB-C2 cells (drug-resistant carcinoma cells) by auraptene and nobiletin has also been reported (29). Other research indicated the *in vitro* and *in vivo* potency of flavonoid dimers on P-gp modulatory properties along with low adverse effects (30). Among biflavonoid structures, rutin has been identified as a potential chemo-sensitizing agent to overcome MDR in cancer (8). Hydrophobic groups of flavonoids are determinant structural fragments for providing P-gp blocking activity since transmembrane helices of P-gp binding pocket mainly consist of hydrophobic and aromatic residues (31,32). Moreover, pairwise energy decomposition analysis (33) showed that auraptene and 7,4',7'',4'''-tetra-O-methylamentoflavone were better M-site binders in comparison to the verapamil ( $\Delta G_b$  of -7.55 kcal/mol). It should be noted that our estimated binding score for verapamil was in good agreement with the previously reported data ( $\Delta G_b$  of -7.60 kcal/mol) (27).

Hoehchst 33342 and rhodamine-123 were considered standard binders to H and R sites, respectively. Ferreira *et al.* proposed a required cut-off threshold as the minimum binding energy of P-gp substrates (-7.00 kcal/mol) (27). According to this criterion, all the phytochemicals except for auraptene and 7,4',7'',4'''-tetra-O-methylamentoflavone may be classified as non-substrates. The low binding energy of diallyl sulfide might be correlated to

the previous results that showed sulforaphane and diallyl sulfide did not affect the cellular accumulation of daunorubicin in P-gp overexpressed drug-resistant KB-C2 cells (34).

### Induced polarity

The best-ranked DFT-based interaction energy was attributed to Phe755 contribution upon binding to auraptene ( $\Delta E_b$  -2.56 kcal/mol). In confirmation of this, our calculation indicated a higher IP value for Phe755 (2.16) concerning Tyr303 (1.39) and Phe331 (1.39). Maximum polarization induction of auraptene structure was obtained for terminal carbon atoms of C9-alkyl substituent (C19 > C21 > C20) (Fig. 7A). These carbon atoms had higher electrostatic contributions toward P-gp. In contrast, chromenone C7 was the least electrostatically induced atom of auraptene. This atom did not show any interactions with auraptene structure (Fig. 2). As pointed out above, in the case of Tyr303, the total IP value was lower than Phe755. Upon binding to Tyr303, C19, and C20 were again the most polarized atoms of auraptene but C21 was not as polarized as before. In overall, our B3LYP level of calculation showed higher polarizability of the auraptene alkyl chain in the presence of Phe755 than Tyr303.

Increased IP values were estimated for those amino acids that made H-bonds to the P-gp binding site. 7,4',7'',4'''-tetra-O-methylamentoflavone had a few polar interactions to R-site. DFT calculations revealed that Tyr303 and Gln721 made energy-favorable hydrogen interactions to 7,4',7'',4'''-tetra-O-methylamentoflavone (Fig. 3). But what about IP of hydrophobic contributions? To answer this question, the electrostatic nature of hydrophobic forces must be taken into account. These contacts are caused by correlations in the fluctuating polarizations of nearby particles. In accordance with the  $\pi$ -stacking interaction between Tyr303 side chain phenyl and central phenyl ring of the ligand, interacted carbon atoms (C12-17; atomistic IPs 0.21-0.40; Fig. 7B) had the highest IP values among all the atoms of 7,4',7'',4'''-tetra-O-methylamentoflavone. Furthermore; the H-bond between Tyr303 side chain hydroxyl and ligand methoxy oxygen could be better

illustrated through induced polarization of O18 (Atomistic IP 0.15). Declined IP values were related to the H-bond interaction between Gln721 and O11 (atomistic IP 0.08). This result might indicate the dominant role of hydrophobic contacts in the binding interaction of Gln721 to 7,4',7'',4'''-tetra-O-methylamentoflavone within the communal region of R and M-sites.

### Conformational variation

Estimated instability energies could be interpreted *via* noticeable changes in dihedral angles. Auraptene tolerated a major torsional shift within the alkyl substituent in order to be accommodated in P-gp M-site. For instance, a C9-O12-C13-C14 dihedral exhibited 138.342° angular rotation. Moreover; additional rotations in other dihedral angles of alkyl substituent afforded an appropriate orientation to make several binding contributions to P-gp hydrophobic residues (Fig. 8). It was clearly observed that the aforementioned dihedral shifts disturbed the coplanarity of chromene ring with regard to the C13-C16 segment of alkyl substituent.

As illustrated before, 7,4',7'',4'''-tetra-O-methylamentoflavone gained 6.7 kcal/mol instability upon binding to P-gp. Inspection of binding poses showed significantly less conformational variations between unbound and docked states when compared to auraptene. Tyr303 has been indicated as an effective binder ( $\Delta E_b$  of -4.82 kcal/mol). In this regard, DFT-based calculations showed a mere rotation of 4.406° around a C12-C13-O18-C19 dihedral to make an H-bond between methoxy and Tyr303 side chain hydroxyl. The terminal methoxy phenyl ring exhibited a 40.062° rotation around the O10-C7-C37-C42 dihedral. New orientation might have a determinant role in making energy-favored hydrophobic contacts to Phe724 ( $\Delta E_b$  of -2.15 kcal/mol). It might be plausible that functional groups being involved in key interactions with receptors, exhibited higher conformational changes.

## CONCLUSION

It has been well documented that resistant cancer cells may be re-sensitized toward

chemotherapeutic drugs *via* inhibition/modulation of P-gp binding sites. Within the current study, fast and robust computational techniques were consecutively utilized to explore the P-gp binding capability of a few highly consumed dietary phytochemicals. Molecular docking simulation and DFT calculations showed a dominant role of P-gp M-site in binding to auraptene. It seemed that auraptene/P-gp complex was mediated through the contribution of hydrophobic and aromatic residues of the M-site. 7,4',7'',4'''-tetra-*O*-methylamentoflavone was another top-ranked binder with prior accommodation inside the P-gp communal modulatory/substrate site. Blind docking scores for best-ranked phytochemicals were superior to verapamil and rhodamine-123 as standard P-gp modulators and substrates, correspondingly. Pairwise amino acid decomposition on the basis of preferentially docked conformations revealed Tyr303 as an important residue of P-gp in binding to studied phytochemicals. Induced polarizability results confirmed larger electrostatic effects for amino acids with energy-favored binding interactions. Conformational analysis of best-ranked phytochemicals exhibited that auraptene and 7,4',7'',4'''-tetra-*O*-methylamentoflavone might not necessarily interact with P-gp binding sites through minimum energy conformations. Obtained results may assist to identify natural MDR reversal agents among highly consumed dietary phytochemicals with potencies to bind to P-gp structure and hence cause tumor chemosensitizing effects.

#### **Acknowledgments**

This work was financially supported by the Ardabil University of Medical Sciences under Grant No. IR.ARUMS.REC.1400.304.

#### **Conflicting interest statements**

The authors declared no conflict of interest in this study.

#### **Authors' contributions**

N. Razzaghi-Asl contributed to the conceptualization of the study; data collection and analysis were performed by N. Razzaghi-Asl, N. Rajaei, and Gh. Rahgouy; N. Panahi and Gh. Rahgouy prepared the first draft

of the manuscript; N. Razzaghi-Asl and N. Rajaei revised the first draft of the manuscript. All authors read and approved the finalized article.

## **REFERENCES**

1. Szakács G, Váradi A, Ozvegy-Laczka C, Sarkadi B. The role of ABC transporters in drug absorption, distribution, metabolism, excretion and toxicity (ADME-Tox). *Drug Discov Today*. 2008; 13(9-10):379-393. DOI: 10.1016/j.drudis.2007.12.010.
2. Heming CP, Muriithi L, Macharia LW, Filho PN, Moura-Neto V, Aran V. P-glycoprotein and cancer: what do we currently know? *Heliyon*. 2022;8(10):e11171,1-9. DOI: 10.1016/j.heliyon.2022.e11171.
3. Mashayekhi SO, Sattari MR, Routledge PA. Evidence of active transport involvement in morphine transport *via* MDCKII and MDCK-PGP cell lines. *Res Pharm Sci*. 2010;5(2):99-106. PMID: 21589798.
4. Tinoush B, Shirdel I, Wink M. Phytochemicals: potential lead molecules for MDR reversal. *Front Pharmacol*. 2020;11:832,1-35. DOI: 10.3389/fphar.2020.00832.
5. Qian J, Xia M, Liu W, Li L, Yang J, Mei Y, *et al*. Glabridin resensitizes p-glycoprotein-overexpressing multidrug-resistant cancer cells to conventional chemotherapeutic agents. *Eur J Pharmacol*. 2019;852:231-243. DOI: 10.1016/j.ejphar.2019.04.002.
6. Marques SM, Šupolíková L, Molčanová L, Šmejkal K, Bednar D, Slaninová I. Screening of natural compounds as P-glycoprotein inhibitors against multidrug resistance. *Biomedicines*. 2021;9(4):357,1-22. DOI: 10.3390/biomedicines9040357.
7. Mesgari Abbasi M, Valizadeh H, Hamishehkar H, Zakeri Milani P. Inhibition of P-glycoprotein expression and function by anti-diabetic drugs gliclazide, metformin, and pioglitazone *in vitro* and *in situ*. *Res Pharm Sci*. 2016;11(3):177-186. PMID: 27499787.
8. Silva N, Salgueiro L, Fortuna A, Cavaleiro C. P-glycoprotein mediated efflux modulators of plant origin: a short review. *Nat Prod Commun*. 2016;11(5):699-704. PMID: 27319155.
9. Kim TH, Shin S, Yoo SD, Shin BS. Effects of phytochemical P-glycoprotein modulators on the pharmacokinetics and tissue distribution of doxorubicin in mice. *Molecules*. 2018;23(2):349,1-14. DOI: 10.3390/molecules23020349.
10. Mohana S, Ganesan M, Agilan B, Karthikeyan R, Srithar G, Beulah Mary R, *et al*. Screening dietary flavonoids for the reversal of P-glycoprotein-mediated multidrug resistance in cancer. *Mol BioSyst*. 2016;12(8):2458-2470. DOI: 10.1039/c6mb00187d.

11. Kushwaha PP, Maurya SK, Singh A, Prajapati KS, Singh AK, Shuaib M, et al. Bulbine frutescens phytochemicals as novel ABC-transporter inhibitors: a molecular docking and molecular dynamics simulation study. *J Cancer Metastasis*. 2021;7:2,1-13. DOI: 10.20517/2394-4722.2020.92.
12. Ganesan M, Kanimozhi G, Pradhapsingh B, Khan HA, Alhomida AS, Ekhzaimy A, et al. Phytochemicals reverse P-glycoprotein mediated multidrug resistance via signal transduction pathways. *Biomed Pharmacother*. 2021;139:111632,1-10. DOI: 10.1016/j.biopha.2021.111632.
13. Pacheco PA, Louvandini H, Giglioti R, Wedy BCR, Ribeiro JC, Verissimo CJ, et al. Phytochemical modulation of P-Glycoprotein and its gene expression in an ivermectin-resistant *Haemonchus contortus* isolate *in vitro*. *Vet Parasitol*. 2022;305:109713. DOI: 10.1016/j.vetpar.2022.109713.
14. Lomovskaya O, Bostian KA. Practical applications and feasibility of efflux pump inhibitors in the clinic: a vision for applied use. *Biochem Pharmacol*. 2006;71(7):910-918. DOI: 10.1016/j.bcp.2005.12.008.
15. Mora Lagares L, Novič M. Recent advances on P-glycoprotein (ABCB1) transporter modelling with *in silico* methods. *Int J Mol Sci*. 2022;23(23):14804. DOI: 10.3390/ijms232314804.
16. Mamizadeh R, Hosseinzadeh Z, Razzaghi-Asl N, Ramazani A. *In silico* analysis of a few dietary phytochemicals as potential tumor chemo-sensitizers. *Struct Chem*. 2018;29:1139-1151. DOI: 10.1007/s11224-018-1098-0.
17. Gontijo VS, Dos Santos MH, Viegas C Jr. Biological and chemical aspects of natural biflavonoids from plants: a brief review. *Mini Rev Med Chem*. 2017;17(10):834-862. DOI: 10.2174/1389557517666161104130026.
18. Daina A, Michielin O, Zoete V. SwissADME: a free web tool to evaluate pharmacokinetics, drug-likeness and medicinal chemistry friendliness of small molecules. *Sci Rep*. 2017;7:42717,1-13. DOI: 10.1038/srep42717.
19. Nicklisch SC, Rees SD, McGrath AP, Gökirmak T, Bonito LT, Vermeer LM, et al. Global marine pollutants inhibit P-glycoprotein: environmental levels, inhibitory effects, and cocrystal structure. *Sci Adv*. 2016;2(4):e1600001,1-12. DOI: 10.1126/sciadv.1600001.
20. Morris GM, Huey R, Lindstrom W, Sanner MF, Belew RK, Goodsell DS, et al. AutoDock4 and AutoDockTools4: automated docking with selective receptor flexibility. *J Comput Chem*. 2009;30(16):2785-2791. DOI: 10.1002/jcc.21256.
21. Morris GM, Goodsell DS, Halliday RS, Huey R, Hart WE, Belew RK, et al. Automated docking using a Lamarckian genetic algorithm and an empirical binding free energy function. *J Comput Chem*. 1998;19:1639-1662. DOI:10.1002/(SICI)1096-987X(19981115)19:14<1639::AID-JCC10>3.0.CO;2-B.
22. Salentin S, Schreiber S, Haupt VJ, Adasme MF, Schroeder M. PLIP: fully automated protein-ligand interaction profiler. *Nucleic Acids Res*. 2015;43(W1):W443-W447. DOI: 10.1093/nar/gkv315.
23. Fogarasi G, Zhou X, Taylor PW, Pulay P. The calculation of *ab initio* molecular geometries: efficient optimization by natural internal coordinates and empirical correction by offset forces. *J Am Chem Soc*. 1992;114:8191-8201. DOI: 10.1021/ja00047a032.
24. Frisch MJ, Trucks GW, Schlegel HB, Scuseria GE, Robb MA, Cheeseman JR, et al. Gaussian, Inc., Pittsburgh PA, USA;1998. Available from: <https://gaussian.com/glossary/g98/>.
25. Mulliken RS. Electronic population analysis on LCAO-MO molecular wave functions. *J Chem Phys*. 1955;23(10):2343-2346. DOI: 10.1063/1.1740588.
26. Shapiro AB, Ling V. Positively cooperative sites for drug transport by P-glycoprotein with distinct drug specificities. *Eur J Biochem*. 1997;250(1):130-137. DOI: 10.1111/j.1432-1033.1997.00130.x.
27. Ferreira RJ, Ferreira MJ, dos Santos DJ. Molecular docking characterizes substrate-binding sites and efflux modulation mechanisms within P-glycoprotein. *J Chem Inf Model*. 2013;53(7):1747-1760. DOI: 10.1021/ci400195v.
28. Takanaga H, Ohnishi A, Yamada S, Matsuo H, Morimoto S, Shoyama Y. Polymethoxylated flavones in orange juice are inhibitors of P-glycoprotein but not cytochrome P450 3A4. *J Pharmacol Exp Ther*. 2000;293(1):230-236. PMID: 10734174.
29. Nabekura T, Yamaki T, Kitagawa S. Effects of chemopreventive citrus phytochemicals on human P-glycoprotein and multidrug resistance protein 1. *Eur J Pharmacol*. 2008;600(1-3):45-49. DOI: 10.1016/j.ejphar.2008.10.025.
30. Cui J, Liu X, Chow LMC. Flavonoids as P-gp inhibitors: a systematic review of SARs. *Curr Med Chem*. 2019;26(25):4799-4831. DOI: 10.2174/0929867325666181001115225.
31. Bai J, Zhao S, Fan X, Chen Y, Zou X, Hu M, et al. Inhibitory effects of flavonoids on P-glycoprotein *in vitro* and *in vivo*: food/herb-drug interactions and structure-activity relationships. *Toxicol Appl Pharmacol*. 2019;369:49-59. DOI: 10.1016/j.taap.2019.02.010.
32. Aller SG, Yu J, Ward A, Weng Y, Chittaboina S, Zhuo R, et al. Structure of P-glycoprotein reveals a molecular basis for poly-specific drug binding. *Science*. 2009;323(5922):1718-1722. DOI: 10.1126/science.1168750.
33. Miri R, Razzaghi-asl N, Mohammadi MK. QM study and conformational analysis of an isatin Schiff base as a potential cytotoxic agent. *J Mol Model*. 2013;19(2):727-735. DOI: 10.1007/s00894-012-1586-x.
34. Nabekura T, Kamiyama S, Kitagawa S. Effects of dietary chemopreventive phytochemicals on P-glycoprotein function. *Biochem Biophys Res Commun*. 2005;327(3):866-870. DOI: 10.1016/j.bbrc.2004.12.081.